Available online at www.sciencedirect.com

ScienceDirect

Procedia Manufacturing 13 (2017) 251–258

Procedia MANUFACTURING

www.elsevier.com/locate/procedia

Manufacturing Engineering Society International Conference 2017, MESIC 2017, 28-30 June 2017, Vigo (Pontevedra), Spain

Feasibility of manufacturing low aspect ratio parts of PLA by ultrasonic moulding technology

U. Heredia[a], E. Vázquez[a], I. Ferrer[b], Ciro A. Rodríguez[a], J. Ciurana[b]

[a] *Tecnológico de Monterrey, Av. Eugenio Garza Sada #2501 Sur, Monterrey, N.L. 64849, México.*
[b] *Department of Mechanical Engineering and Industrial Construction. University of Girona. C/Maria Aurèlia Campany,61,Girona 17071, Spain.*

Abstract

Ultrasonic moulding is a promising technology capable of producing complex mini and micro components highly demanded both electronical and medical sectors. This research work presents a preliminary study to evaluate the feasibility of producing low aspect ratio parts of polylactide acid (PLA) by ultrasonic moulding process. Additionally, mould design considerations are presented to increase literature regarding USM tooling. Finally, some moulding trials were performed to demonstrate the process feasibility to obtain parts fulfilling dimensional requirements.

Peer-review under responsibility of the scientific committee of the Manufacturing Engineering Society International Conference 2017.

Keywords: Ultrasonic moulding process, mould design, mould simulation, low aspect ratio, micro parts

1. Introduction

Ultrasonic moulding process (USM) is a novel technology created to produce micro components with weights lighter than one gram. USM process can be used to mold complex 3D micro parts with a wide variety of polymeric materials. Here the ultrasonic vibration energy is applied by a sonotrodo to heat and plasticized the polymeric material, different to the conventional injection process, where frictional and thermal energy is applied to heat the material by means of a reciprocated screw.

* Corresponding author. Tel.: +0-000-000-0000 ; fax: +0-000-000-0000 .
E-mail address: ines.iferrer@udg.edu

2351-9789
Peer-review under responsibility of the scientific committee of the Manufacturing Engineering Society International Conference 2017.
10.1016/j.promfg.2017.09.065

According Grabalosa et al.[1] the process can be divided in four phases: feeding, vibration initiation, filling and packing and cooling phase. First, in feeding stage, the thermoplastic material is introduced in pellets form inside of a plasticization chamber which is formed by the two halves of the mould used in the process. Then, in vibration initiation stage, the sonotrode moves down until the tip reaches the pellets and starts to vibrate at a specified frequency producing ultrasonic waves that heat the material and starting to melt it. The sonotrode remains vibrating at the top of the plasticization chamber while the plunger located at the bottom of the chamber is used to inject the melted material through the runners until the cavity mould. Finally, a packing and cooling phase is required giving the final properties and dimensions of the moulded part. At the end, the sonotrode returns to its initial position and the mould is opened to extract the moulded part. In this step the plunger helps to demould the part. Unlike the process description introduced in [1-3], the only difference with the above explanation is that in the sonotrode pushes the melted material while the plunger remains in a particular position in the bottom plate during the injection phase.

There are in the literature several studies related to this technology. Michaeli et al. [4] developed a platform to prove the micro injection capabilities of USM. Effects of process parameters also was studied on polypropylene (PP), polyoxymethylene (POM), and polypropylene using blue and yellow master batches. Planellas et al. [5] found out that ultrasonic energy mixes in a homogenous way a dispersion nanoclays in a polylactide (PLA) and polybutylene succinate (PBS) matrices. High orientation of clay nanosheets was found in the direction of polymer flow too. In other words, the ultrasonic moulding brings out the possibility to prepare nanocomposites materials based in polymer matrices. Sacristán et al. [6] studied the effects of ultrasonic moulding on the chemical and mechanical properties of PLA specimens founding a degree of material degradation due to the amount of applied ultrasonic energy, making evident the importance of process parameters. Grabalosa et al [1] researched about design considerations of a stepped sonotrode. They developed a sonotrode operating frequencies map with the aim to increase sonotrode life cycle. Recently Negre et al. [3] studied the ultrasonic moulding process parameters for manufacturing polypropylene parts.

As an emerging technology, there is a limited literature regarding the design and fabrication of tooling and how the filling behaviour is influenced by part geometry. In this last issue several simulations about the heat generation mechanisms performed in the USM process have been developed [7]-[8]. However filling behaviour simulations haven't been studied yet. In [9] a commercial injection moulding simulation software (Autodesk® Moldflow®) was used to improve part quality and process parameters optimization of a PLA micro-stitch used in medical applications. Furthermore, Estrada et al.[10] presented a micro moulding case study of a locking ligation system , where they incorporated preliminary simulations of this Autodesk® Moldflow® to develop a methodology to design and manufacturing micro-cavities for micro moulded parts.

Therefore, the aim of this research work is to provide a preliminary study to evaluate the feasibility of producing low aspect ratio PLA plates by ultrasonic moulding process. Additionally, mould design considerations are presented to increase literature regarding USM tooling. Finally, some moulding trials were performed to validate mould functionality with a quality and dimensional approach.

2. Research method

The target geometry is a rectangular part of 20x25 mm and a thickness of 400 μm, therefore having a low aspect ratio part of 0.0125. The raw material used for the experiments is Ingeo™ Biopolymer 3251D (PLA) from NatureWorks. Considering this target geometry, the methodology is broken down into four steps (see Fig.1).

2.1. Moldflow simulation.

Autodesk® Moldflow® Adviser student version was used to simulate the filling process and to compare it with experimental trails. The part filling, air tramps location and the frozen layer fraction were analyzed. Ingeo Biopolymer 3251D (Commercial name) was chosen as the processing material. This simulation was performed considering the next assumptions: i) the polymer is injected at 190°C and it is completely melted while the mould temperature was setup to 45°C, ii) the injection moulding machine can reach up to 180 MPa of injection pressure, and iii) dual domain mesh type resulting: 4716 CAD triangles and 2360 CAD nodes generated.

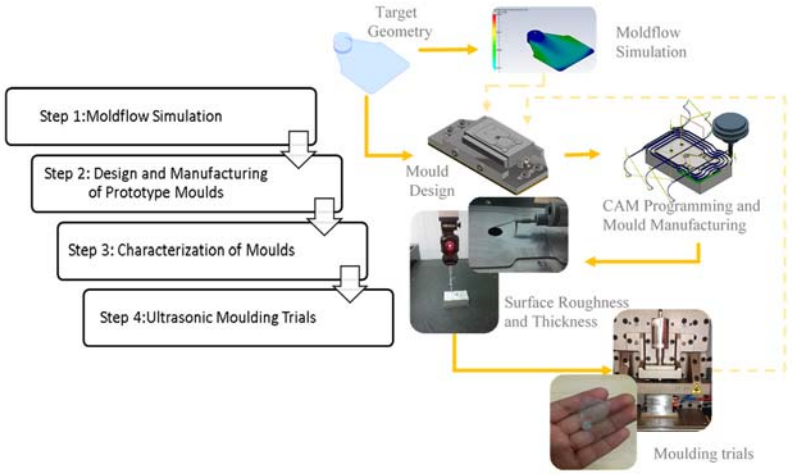

Fig. 1. Methodology route map.

2.2. Design and manufacturing of prototype moulds.

Mould design considerations were taken from microinjection moulds and conventional injection moulding literature. Fig. 2 shows the entire mould assembly designed and manufactured to carry out injection trails. There is a cavity insert because different mould layouts were tested reducing additional effort and cost. To reduce mould complexity additional ejection pins were not included.

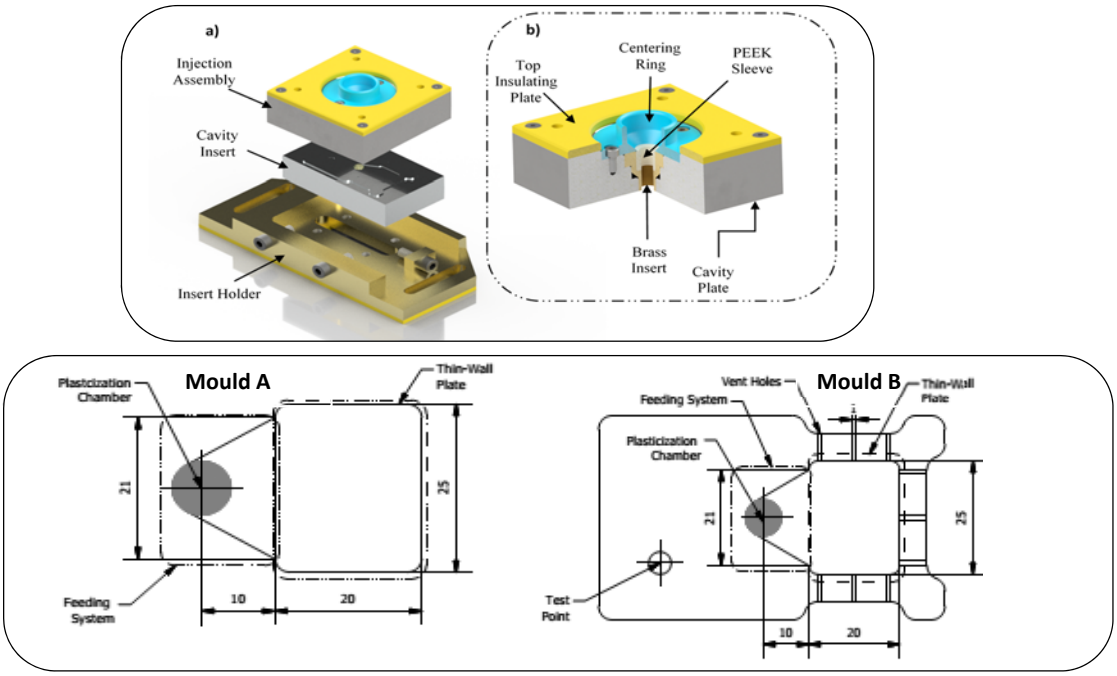

Fig. 2. Mould assembly and layout mould configurations.

Furthermore, two different mould inserts were manufactured to study the vent holes influence on the filling of the moulded parts. Both mould inserts (A and B) were designed with a direct fan gate and the parting line placed at the top surface of the target geometry. The dimensions of the vent holes machined in the B mould insert was 1 mm width

and 25µm height. Furthermore, a peripheral contour was machined to reduce flatness error caused by machine setup and focalize clamp force in a small area around the cavities (Fig. 2).

The experimental setup for manufacturing the mould is described in Table 1. Micro milling techniques and tools were used to manufacture mould cavities and the vent holes. Tool length was measured manually inside the machine and preliminary test machining circular pockets of 5 mm diameter and 50µm were machined to evaluate the Z-axis accumulated error from different sources such as the tool length measurement, thermal dilatation of the machine spindle and setup of the clamping system.

Table 1. Machining setup.

Resource	Description
CAM Software	Autodesk® HSM® Student Version 2017.
Machine tool	Deckel-Maho 64V Linear with positioning accuracy of 20 and 10 µm in Y and Z directions respectively, and 8µm in X direction. Spindle speed up to 12,000 rpm
Clamp System	Standard clamp holder, setup flatness error was ± 5 µm.
Dial indicator	Mitutoyo Dial Indicator with graduation of 1µm and accuracy of ± 5 µm.
Cutting tools	HOLEX solid carbide mini slot drill 1 mm diameter used to machine vent holes.

2.3. Characterization of the moulds.

Measurement of surface roughness at bottom surface was conducted with a stylus instrument Mitutoyo SV2000 Surftest considering three longitudinal sections across the mould cavities. Thickness and width measurements of the mould cavities were conducted using the Mitutoyo Crystal-Apex C Coordinate Measuring Machine with an accuracy of ±1µm. Additionally, parallelism between mould parting surface and cavity bottom& mould parting surface flatness were also measured using the same measuring instrument. The thickness and width measurements were used to determine with more accuracy the expected part mass (without considering shrinkage) and moulded part thickness.

2.4. Ultrasonic molding experiments.

The experimental phase was divided in two stages. In the first one, the objective was study the influence of each mould insert in filling cavity (Table 2). In the second one, the objective was to analyze the influence of the preliminary compaction and the ultrasound time on dimensional accuracy and part weight. The fixed parameters were 14 pellets per shot (it is around 551.83 mgr. with a standard deviation of 12.014 mgr.), cooling time, force, amplitude and velocity (Table 2).

The issues measured in the obtained parts are filling part, mass and dimensional accuracy, considering the thickness and width. The filling part was quantified by complete or incomplete parts. On the other hand, the thickness were measured in five different areas to observe thickness variation through the moulded part using. The Micromar 40 EWV micrometre with accuracy of ±1µm was used. The mass of the moulded test parts was measured used a KERN Precision Balance with readability of 0.001 gr, and next compared with the expected mass considering real mould dimensions. This measured mass included both the moulded part and the gate. Finally, the width of all the moulded parts were measured using the same CMM used to measure the cavity width of each mould. White zones within the samples were observed with Nikon SMZ-745T stereomicroscope.

Table 2. Process Conditions: first stage and second stage.

	Process Condition	Trails	Mold insert	Force (N)	Amplitude (%)	Ultrasound time (s)	Velocity (mm/s)	Cooling time (s)	Preliminary compaction
First stage	1	10	A	2000	0.6	2.6	4	15	No
	2	10	B	2000	0.6	2.6	4	15	No
Second stage	3	10	B	2000	0.6	3	4	15	Yes
	4	10	B	2000	0.6	2.75	4	15	No

3. Results and discussion

3.1. Simulation results.

The filling confidence graph displays the filling probability within the cavity considering conventional injection moulding conditions. Fig. 5.a shows that the part has a high probability of filling (99.8%) but it results on a short shot or incomplete part. Due to the large surface area and its narrow thickness, that causes a huge heat loss in contact with the mould. Unlike simulation results, complete parts were obtained during moulding trials as depicted in Fig. 5.d and 5.e. Complete moulded parts indicated that ultrasonic waves during the injection phase improved the cavity filling. Air traps graph (Fig. 5.b) displays all those zones with high probability to contain air traps. Fig. 5.d pictures the convergence of flow fronts which promote air traps formation. To avoid air traps one of the proposed moulds incorporated vent holes in those critical areas of the cavity. On the other hand, the frozen graph (Fig. 5.c) displays high fraction values of the frozen layer in the side walls and lower values in the centre. The frozen layer is highly related to flow resistance through the part. As the frozen layer increases the thickness of the flow layer decreases affecting flow resistance and filling. Fig. 5d presents a comparison between the expected laminar flow with the real and turbulent plastic flow during trials. Thus, this turbulent flow should be considered when is performing USM simulations to obtain more precise results. Additionally, Fig. 5.e shows that in the most of the complete parts appeared white filled with micro-bubbles when the specimens were observed through a microscope.

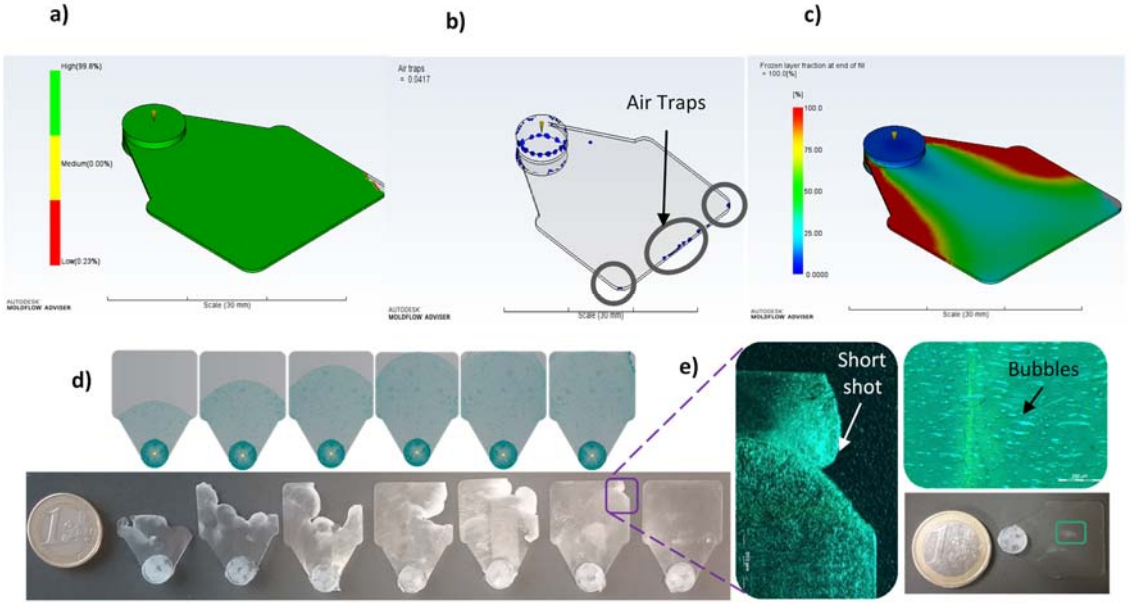

Fig. 5. Simulation results: a) filling confidence, b) air traps, c) frozen layer, d) simulated and real polymer flow, e) short shot and bubbles.

3.2. Design and manufacturing of prototype moulds.

The full mould assembly was successfully machined and installed in the USM machine. Fig. 6 shows the mould partially assembled and the finished mould inserts. Strong concentricity requirements of all the components was achieved avoiding sonotrode collisions with the insert brass walls and therefore preventing the sonotrode wear and part contamination with brass particles. Closed tolerances of the PEEK sleeve reduce alienation problems and reduce melted material leaks when both the processing pressures are the index flow of the injected material are high.

Fig. 6. Tooling prepared to perform moulding trials.

3.3. Characterization of moulds.

The average thickness of both mould is arround 405 µm, ± 1µm therefore machining difference have a neglectable effect over the results. The width of B mould insert was 25.098 ±1µm. Besides that, surface roughness is considered an important parameter when mould surface quality is evaluated based on the final product requirements. Furthermore, in [11], there is experimental research that points out that lower surface roughness mould finishes generate higher turbulence in the polymer flow than higher surface roughness mould finishes, therefore improving the mixing effect in the mould. Regarding the surface roughness of both insert A and insert B, Ra values of 0.360 µm and 0.269 µm were obtained respectively. Surface roughness variation in the three sections was due to morphology of the pocket strategy used to machine the cavities.

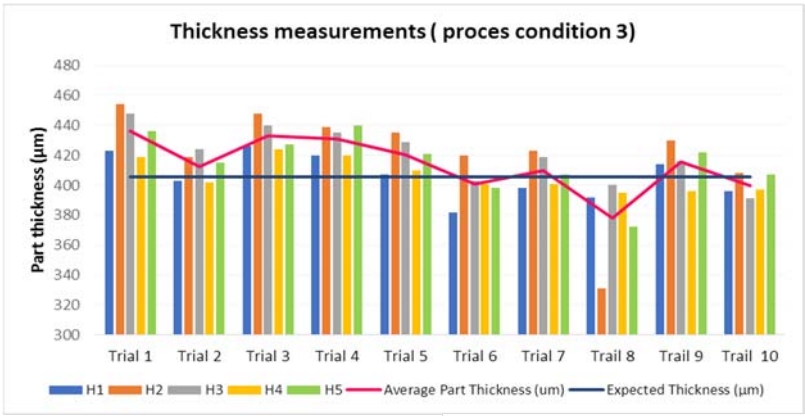

(a)

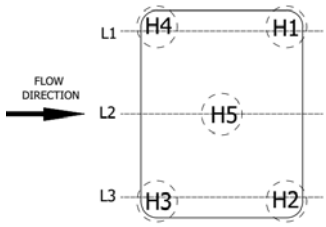

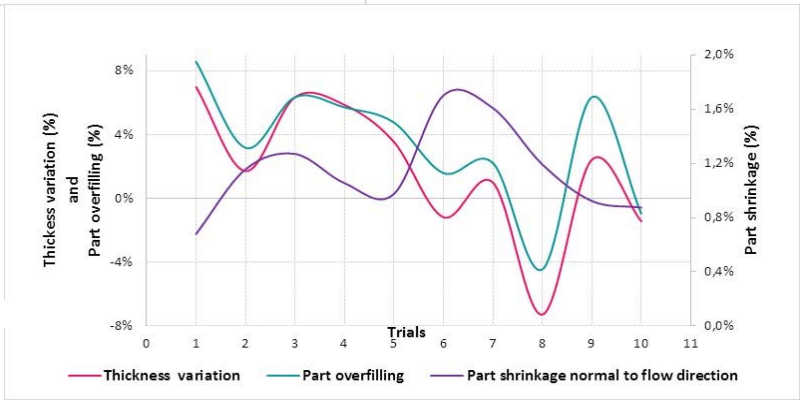

(b)

Fig. 7. Process conditions 3: a) thickness measurements of moulding trials; b) thickness variation, part shrinkage and part overfilling

3.4. Ultrasonic moulding trials.

Actually, the use of vent holes in ultrasonic moulding of low aspect ratio parts increases the number of complete moulded parts from 20% to 70% (from 2 to 7 over 10 trails obtained to each condition). As notice, trapped air inside the cavity increases the flow resistance causing a short shot. Moreover, the vent holes improve the cavity filling because the vent holes reduce interior mould cavity pressure letting out the air and gases produced inside of the cavities. Furthermore, no flash around the cavities was not visualized.

Fig. 7 (a) plots the result of thickness measurements of the process condition 3 in five different sections of each part. The results reveal the H2, H3 and H5 sections being thicker than H1 and H4 sections. Really, H2 and H3 region have highest thickness values in more than the 50% of the trails. Analyzing the mould dimension, it would expect to be H1 and H2 the thicker ones, due to their highest dimensions. However, this deviation could be caused by the location of the thermal resistant in this area. Thus, higher thermal energy has been storage by the material leading to liberate more energy during the demoulding processes which increase the material volume. Moreover, in general, most of the thickness are higher than the theoretical dimension, phenomenon no common in microinjection moulding. However, considering the high values of energy that the material receive during the process the energy liberation when the mould open could be a reasonable reason. Fig. 8 (b) is a complementary graph where it is plot thickness variation, part overfilling and part shrinkage. The part overfilling was calculated comparing both the specimen and theoretical mass, whereas the shrinkage was calculated using the width dimension. As expected, the thickness and the overfilling have the same trend. As thicker the part is, heavier it becomes. On the contrary, the shrinkage increase when the thickness and the weight decrease.

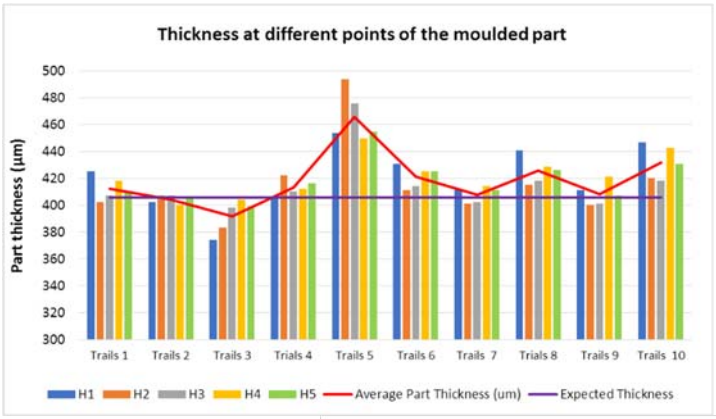

a)

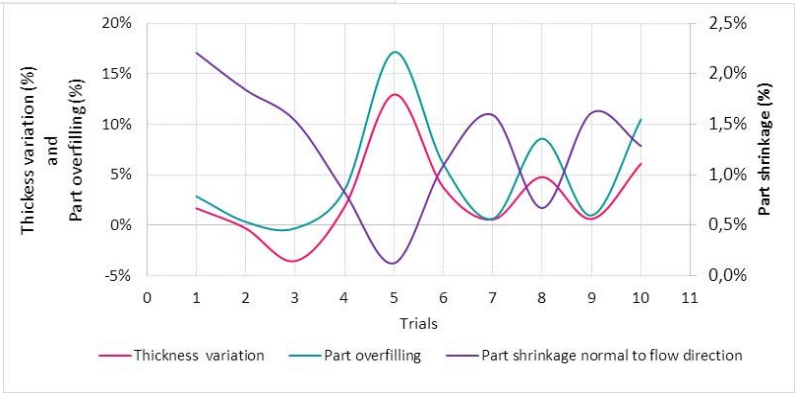

b)

Fig. 8. Process conditions 4: a) Thickness variation; b) Thickness, shrinkage and part overfilling

Fig. 8 represents the results for process conditions number 4 (Table 2). Here the areas H1 and H4 were higher in the 60% of the cases, the opposite side that the process conditions 3. On reasonable reason could be the location of the resistant, which in that case was located in this side. In the same way therefore, the trend of the thickness, the

overfilling and shrinkage is the same than Fig. 7. As thicker the part is, heavier it becomes, and the shrinkage increase when both decrease.

The part filling, in both moulds, can be affected by some process parameters not controllable during the manufacturing process, such as the sonotrode temperate or the PEEK sleeve wear. When the peek sleeve is well manufactured and without wear, it is possible to get complete moulded parts without vent holes, but once the PEEK sleeve become looser, the melt flows upward of the injection assembly produces short shots. The resulted flow layer is too narrow that requires high injection pressures to fill the cavity, even in some cases the frozen layer is almost the whole thickness of the moulded part restricting the polymer flow to the end of the cavity. Part overfilling could be explained due to the lack of the homogeneity of PLA pellets (14 pellets per trial) which make vary the mass in each cycle, which could be avoided using a stricter dosage control. The observed trend about the shrinkage reduction with an increase of mass in the moulded part is consistent with literature.By other hand, part thickness dilatation effect could be caused by a premature part ejection and high residual stresses in the part. During the mould setup stage, heating resistors were placed in different positions in process condition 3 and 4, staying closer to points H2 and H3 in process condition 3, while in process condition 4 were closer to H1 and H4. This issue could has influenced in the thickness variations and polymer flow.

4. Conclusions

This work demonstrated the feasibility of producing low aspect ratio part of PLA by means of ultrasonic microinjection moulding techniques. It has been observed that the use of commercial injection moulding simulation software provides a preliminary idea of the feasibility of part filling, even it can be used to identify those areas with air traps improving mould design incorporating vent holes close to them. Furthermore, the use of vent holes was evaluated demonstrating improvement in part filling without generating flash. Further work will be conducted increasing dosage control and mould heating testing more biopolymers and reducing part thickness.

Acknowledgements

The author thanks the Mexican National Science and Technology Council (CONACyT)

References

[1] J. Grabalosa, I. Ferrer, O. Martínez-Romero, A. Elías-Zúñiga, X. Plantá, F. Rivillas, J. Mater. Process. Technol. 229 (2016) 687–696.
[2] J. Grabalosa, I. Ferrer, A. Elías-Zúñiga, J. Ciurana. Mater. Des. 98 (2016) 20–30.
[3] P. Negre, J. Grabalosa, I. Ferrer, J. Ciurana, A. Elías-Zúñiga, F. Rivillas. MESIC Manuf. Eng. Soc. Int. Conf. 2015. 132 (2015) 7–14.
[4] W. Michaeli, T. Kamps, C. Hopmann. Microsyst. Technol. 17 (2) (2011) 243–249.
[5] M. Planellas, Ultrason. Sonochem. 21 (4) (2014) 1557–1569.
[6] M. Sacristán, X. Plantá, M. Morell, J. Puiggalí, Ultrason. Sonochem. 21 (1) (2014) 376–386.
[7] W. Wu, H. Peng, Y. Jia, B. Jiang. Microsyst. Technol. (2016) 1–8.
[8] B. Jiang, H. Peng, W. Wu, Y. Jia, Y. Zhang, Polym. 8 (5) (2016) 1–12.
[9] O.C. Gheorghe, T.D. Florin, G.T. Vlad, D.T. Gabriel. 24th DAAAM Int. Symp. Intell. Manuf. Autom. 69 (2013) 340–346.
[10] P. Estrada, H.R. Siller, E. Vázquez, C.A. Rodríguez, O. Martínez-Romero, R. Corona. Second CIRP Conf. Biomanufacturing. 49 (2016) 1–7.
[11] C.A. Griffiths, S.S. Dimov, E.B. Brousseau, R.T. Hoyle. J. Mater. Process. Technol. 189 (1-3) (2007) 418–427.
[12] M. Sorgato, M. Babenko, G. Lucchetta, B. Whiteside. Int. J. Adv. Manuf. Technol. 88 (1) (2017) 547–555.